Environmental Science & Technology

pubs.acs.org/est

Article

Using Potential Molecular Transformation To Understand the Molecular Trade-Offs in Soil Dissolved Organic Matter

Meng Wu, Pengfa Li, Guilong Li, Kai Liu, Guozhen Gao, Shiyu Ma, Cunpu Qiu, and Zhongpei Li*

Cite This: *Environ. Sci. Technol.* 2022, 56, 11827−11834

Read Online

ACCESS | Metrics & More | Article Recommendations | Supporting Information

ABSTRACT: Understanding the chemical composition and molecular transformation in soil dissolved organic matter (DOM) is important to the global carbon cycle. To address this issue, ultrahigh-resolution Fourier transform ion cyclotron resonance mass spectrometry (FT-ICR-MS) was applied to investigate DOM molecules in 36 paddy soils collected from subtropical China. All the detected 7576 unique molecules were divided into seven compound groups, and nine trade-off relationships between different compound groups were revealed based on principal component analysis and Pearson's correlation. An optimized method was developed to evaluate all potential molecular transformations in DOM samples. The concept of thermodynamics was introduced to evaluate the identified molecular transformations and classify them as thermodynamically favorable (TFP) and thermodynamically limited (TLP) processes. Here, we first tried to understand the molecular trade-offs by using the potential molecular transformations. All the nine trade-offs could be explained by molecular transformations. Six trade-offs had bases of biochemical reactions, and the trade-off-related direct transformations could explain the content variations of carbohydrate-like, condensed aromatic-like, tannin-like, and lignin-like compounds in TLP. More reasonable explanations existed in the TLP rather than TFP, which demonstrated the critical role of external energy in the molecular transformation of soil DOM.

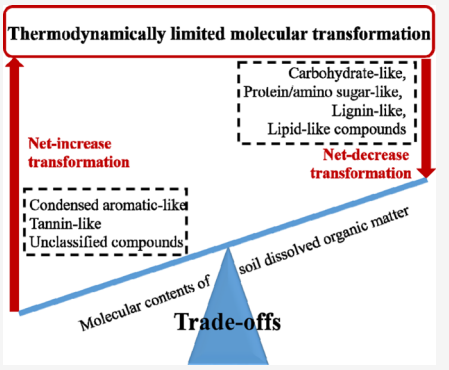

KEYWORDS: *DOM, carbon cycle, molecular transformation, thermodynamically, trade-off, FT-ICR-MS*

INTRODUCTION

The global soil organic carbon (SOC) pool of 1550 gigatons is more than the sum of atmospheric and biotic pools.[1] A framework for predicting the SOC molecular composition could provide understanding of the global carbon cycle. The carbon composition of SOC was found to vary in predictable ways as some trade-off relationships exist among different compounds on a continental scale.[2] The trade-offs between carbohydrate and char, carbohydrate and lipids, and lignin and protein displayed complementary mechanisms of SOC persistence from the view of chemical composition of SOC. Although soil dissolved organic matter (DOM) accounts for only a minor fraction of the global soil carbon, it is the most active organic pool and plays a vital role in the carbon cycle,[3] yet the dynamics of this carbon pool remains elusive. Whether similar trade-off relationships exist in the DOM molecular composition is unknown, and revealing this issue will be helpful to further understand the carbon persistence and transformation.

The carbon cycle inevitably involves changes in the carbon composition and chemical properties. Thus, evaluating the chemical transformation characteristics of DOM is important to understand the carbon cycle. Commonly, the variation in the bulk chemical characteristics of DOM can be evaluated through its spectral features, including fluorescence spectra[4] and ^{13}C nuclear magnetic resonance (NMR) spectra,[5] and some research studied the changes in DOM molecular weights using size-exclusion chromatography to represent the molecular variations as a whole.[6] Until recently, with the advent of high-resolution mass spectrometry, such as ultrahigh-resolution Fourier transform ion cyclotron resonance mass spectrometry (FT-ICR-MS), it was possible to discern the chemical properties of DOM at the molecular level.[7−9] Using this technology, the molecular transformation could be investigated by comparing the molecular characteristics before and after a process. For example, some research studies picked out molecular formulas that were newly formed or removed to represent the transformations.[10,11] Molecular transformations could also be detected through changes in the average molecular weight[12] and oxidation state[13,14] of DOM molecules of the origin and daughter products. However, these characterization methods did not clarify the pairs of molecules in which specific transformations occurred.

Received: February 15, 2022
Revised: July 13, 2022
Accepted: July 14, 2022
Published: July 26, 2022

https://doi.org/10.1021/acs.est.2c01137
Environ. Sci. Technol. 2022, 56, 11827−11834

A recent study employed an effective approach to display the specific molecular transformations in an ultraviolet oxidation process based on 24 types of transformation reactions that have been reported.[15] The key point of the approach is the knowledge of possible removing formulas in the known reactions. If a molecular change between the precursors and products matches a possible removing formula, a specific molecular transformation can be confirmed. Thus, if the possible removing/obtaining molecular formulas during DOM molecular transformations could be known, the potential reactions among all the DOM molecules can be established. Based on a summary of existing biochemical reactions, Graham et al. provided a list of 92 common intermediates of biochemical transformations.[16] Then, the biochemical transformation database was supplemented, and the number of identified transformation intermediates reached 1209.[17] Based on the new transformation database, any between-molecule difference could be tested if it matches a potential biochemical transformation.

As the largest anthropogenic wetlands on earth,[18] paddy fields play an important role in carbon sequestration and greenhouse gas emission.[19,20] However, the dynamics of DOM transformation in paddy soils is poorly understood. In this study, FT-ICR-MS was used to identify the molecular formulas of DOM, and the potential biochemical transformations among all the DOM molecules were investigated. Trade-offs of DOM molecular compositions in paddy soils were evaluated at a regional scale in subtropical China. The relationship between molecular trade-offs and molecular transformations was also studied, and we attempted to explain the trade-offs using molecular transformations.

MATERIALS AND METHODS

Soil Sampling. The experimental sites are located in long-term-operated paddy fields of four cities (Changshu, Jinxian, Wangcheng, and Yingtan) in subtropical China. The straight-line distance between the four experimental sites ranges from 400 to 1350 km (Figure S1). At each site, three typical long-term fertilization treatments were selected: (1) no fertilizers, (2) mineral fertilizers, and (3) mineral fertilizers plus organic amendments. Three replicates for each treatment were sampled at each site. Thus, a total of 36 paddy soil samples (3 treatments × 3 replicates × 4 sites) was collected from this area. All samples were collected approximately 10−20 days after rice harvest. Five cores were taken from the topsoil (0−15 cm) and homogenized to form one composite soil sample. The soil samples were then sieved (<2 mm) for further analysis. A detailed description of the experimental sites and basic chemical properties of the soils are provided in Tables S1 and S2.

DOM Extraction. Soil DOM was extracted with ultrapure water (1:10 w/v) and shaken for 4 h in a horizontal shaker at room temperature. Then, the solutions were centrifuged at 2800*g* for 20 min and filtered through a 0.45 μm membrane filter to obtain the DOM samples.

FT-ICR-MS Test. A detailed description of FT-ICR-MS can be found in a previous study.[21] Briefly, the DOM solution was loaded onto acidified PPL cartridges (Agilent Technologies, Santa Clara, CA, USA) for clean-up and collected from the cartridges using methanol (HPLC grade, Merck, Germany). Then, the DOM elutes were tested using electrospray ionization (ESI) FT-ICR MS equipped with a 9.4T actively shielded superconducting magnet interfaced with a negative-ion mode ESI (Bruker, Billerica, MA, USA). For each DOM sample, deuterated octadecanoic acid (7.5×10^{-3} μmol/L) was added as an internal standard. The samples were injected into the ESI source at a speed of 180 μL/h. The polarization voltage was 4.0 kV, and the capillary column introduction and outlet voltages were 4.5 kV and 320 V, respectively. Ions were accumulated in a hexapole for 0.001 s before being transferred to the ICR cell. The mass-to-charge ratio (m/z) ranges from 150 to 800 Da. A 4M word size was selected for the time domain signal acquisition. The signal-to-noise ratio (S/N) and dynamic range were enhanced through accumulating 128 times domain FT-ICR transients.

FT-ICR-MS Data Processing. The raw FT-ICR-MS spectra were converted to a list of m/z values by a data analysis software (Bruker Daltonics version 4.2) with the following data thresholds: an absolute intensity threshold of 100 and S/N > 6. To reduce cumulative errors, all sample peaks from the entire data set were aligned to each other to eliminate possible mass shifts. Molecular formulas of the mass peaks were calculated using a custom software. The peaks that were taken into consideration for further analysis were those that were observed at least twice among the 36 samples. Based on the obtained molecular formulas, the aromaticity index (AI) and Gibbs free energy for the half reaction of carbon oxidation ($\Delta G0$) of each molecule were calculated using the following equations[22−24]

$$\mathrm{AI} = (1 + a - d - f - 0.5b)/(a - d - f - c - e)$$

$$\Delta G0 = 60.3 - 28.5 \times \mathrm{NOSC}$$

$$\mathrm{NOSC} = -((-Z + 4a + b - 3c - 2d + 5e - 2f)/a) + 4$$

where a, b, c, d, e, and f represent the atom number of the elements C, H, N, O, P, and S (respectively) in a molecular formula; NOSC is the nominal oxidation state of carbon and it could reflect whether the microbial oxidation of organic matter is thermodynamically favorable[25,26] and Z is the corresponding net charge (we assume a neutral charge per molecule). A molecule with a higher $\Delta G0$ value means that the molecule is more thermodynamically unfavorable to be mineralized, that is, more stable at the molecular level.[23]

The thousands of obtained molecular formulas could be categorized into different compound groups according to molecular elemental ratios and AI:[27] (1) condensed aromatic-like (CA) compounds (O/C: 0−0.67, H/C: 0.2−0.7, and AI ≥ 0.67); (2) carbohydrate-like (CH) compounds (O/C: 0.67−1.2 and H/C: 1.5−2.4); (3) lignin-like (LG) compounds (O/C: 0.1−0.67, H/C: 0.7−1.5, and AI < 0.67); (4) lipid-like (LP) compounds (O/C: 0−0.3 and H/C: 1.5−2.0); (5) protein/amino sugar-like (PA) compounds (O/C: 0.3−0.67, H/C: 1.5−2.2, and N/C ≥ 0.05); (6) tannin-like (TN) compounds (O/C: 0.67−1.2, H/C: 0.5−1.5, and AI < 0.67); (7) unsaturated hydrocarbons (UH) (O/C = 0−0.1 and H/C = 0.7−1); and (8) unclassified compounds (UC), the compounds that do not belong to the above groups. In our samples, seven compound groups except UH were detected.

Optimized Identification Method for Transformation between Molecules. According to previous literature studies,[24,28] the potential biochemical transformations between molecules could be picked up based on the mass differences between FT-ICR-MS peaks within each sample. Based on the ultrahigh mass accuracy of FT-ICR-MS, the mass difference

https://doi.org/10.1021/acs.est.2c01137
Environ. Sci. Technol. 2022, 56, 11827−11834

between two peaks could be assigned to specific compounds in the transformation database.[17] For example, a mass of 71.0371 Da represents a reaction in which one alanine (C_3H_5NO) is gained or lost. However, there is a bug in this assigning process. In the above process, an exact mass difference refers to a specific compound or molecular formula (trans-formula) in the database. However, in real situations, a mass may refer to different compounds or molecular formulas. For example, the mass 44.9977 refers to COOH (carboxyl) in the trans-formation database. When we evaluated the potential trans-formations between molecules in this study, we found that the transformation from $C_{17}H_{21}O_{13}S$ (peak m/z: 465.0702) to $C_{22}H_{14}NO_8$ (peak m/z: 420.0725) was assigned to the transformation of COOH lost as their mass difference was 44.9977. Some isotopically labeled molecules might also contribute to such fake transformations, and that could overestimate the actual transformations among the molecules. Thus, the trusted transformation between two molecules should simultaneously meet the following two restrictive conditions: (1) the differential formula between two molecules should have the same mass of a trans-formula in the database and (2) the differences in the number of atoms (C, H, N, O, etc.) between two molecules should have the same number of corresponding atoms in the trans-formula in the database. In this study, we counted the transformations of removing molecular formulas. The transformation was first identified within each sample, and then all the possible unique transformations from all the 36 samples were put together to form a final transformation file. Only considering the mass difference between two peaks that matched with the transformation database, there were 68,113 potential trans-formations among the detected molecules in this study. However, when considering the above two restrictive conditions, 2115 fake transformations were found and filtered out.

The transformation involves not only molecular conversion but also energy changes. With the transformation of molecules, the Gibbs free energy for the half reaction of carbon oxidation ($\Delta G0$) also changed. The value of the energy change (ΔG) is defined as follows:

$$\Delta G = \Delta G0_{\text{before}} - \Delta G0_{\text{after}}$$

where $\Delta G0_{\text{before}}$ and $\Delta G0_{\text{after}}$ represent $\Delta G0$ of the molecules before and after the transformation, respectively. If $\Delta G < 0$, the transformation occurred from a compound with low $\Delta G0$ (less stable thermodynamics) to a compound with high $\Delta G0$ (more stable thermodynamics). Thus, the $\Delta G \leq 0$ transformation could happen spontaneously in thermodynamics and could be treated as a thermodynamically favorable process (TFP). In contrast, the $\Delta G > 0$ transformation requires external energy or additional forces and can be treated as a thermodynamically limited process (TLP).

Statistical Analysis. The transformations between any two molecules were first counted based on a previous method[17] (https://github.com/danczakre/Meta-Metabolome_Ecology) using R software (version 4.0.3) and then were further selected by the two restrictive conditions mentioned above. Principal component analysis (PCA) was conducted in R software, and Pearson's correlation was conducted to analyze the statistical significance ($P < 0.05$) using SPSS 19.0 (SPSS Inc., Chicago). The Sankey diagram and heatmap were generated in R software with the "riverplot" and "ggplot2" package, respectively.

RESULTS AND DISCUSSION

Molecular Trade-Offs in Soil DOM at a Regional Scale. For all the DOM samples, a core group of 7576 unique molecules was determined by FT-ICR-MS with molecular masses ranging from 181 to 716 Da. All the molecules were plotted in a van Krevelen diagram with oxygen-to-carbon (O/C) and hydrogen-to-carbon (H/C) element ratios of molecular formulas as the x-axis and y-axis, respectively (Figure 1a). Each point represents a compound, and all the

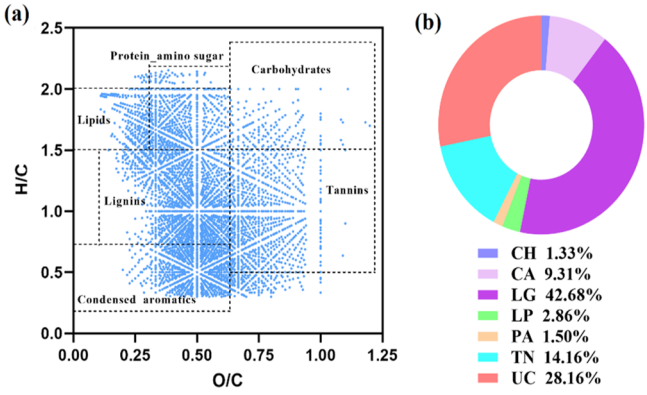

Figure 1. van Krevelen diagrams from the FT-ICR-MS spectra of DOM. (a) Dotted boxes overlain on the plot refer to seven major biomolecular compound groups: carbohydrates (CH), condensed aromatics (CA), lignins (LG), lipids (LP), proteins/amino sugars (PA), tannins (TN), and unclassified compounds (UC). (b) Percentage of the number of compounds in each compound group is presented.

detected compounds were divided into the following seven compound groups: CH, CA, LG, LP, PA, TN, and other UC. Among all the compound groups, LG, UC, and TN were the largest constituents, with mean values of 42.68, 28.16, and 14.16% of all the DOM molecules, respectively (Figure 1b). The readily decomposable compounds CH, LP, and PA only accounted for very small percentages (<3%), while the more stable CA compound group showed a much higher percentage (9.31%). Across all the diverse DOM samples, although the percentages of some specific compounds in different samples showed differences, the relative proportions of different compound groups displayed a consistent variation pattern (Table S3).

Across all the samples, the DOM molecules covaried in predictable ways. PCA based on the percentages of the compound classes showed that the correlation matrix of DOM molecules could be well explained (86.67%) by three axes. On the PC1 axis, PA and CH (Figure 2a), CA and UC (Figure 2a,b), and PA and LP (Figure 2a,b) were positively correlated, while PA and CH were negatively correlated with CA and UC at the PC1 axis (Figure 2a,b), CA was negatively correlated with LG and LP at the PC1 axis (Figure 2a,b), and TN was negatively correlated with LG, LP, and UC at the PC2 axis (Figure 2a,c). Pearson's correlation analysis also showed that PA and CH, PA and LP, and CA and UC were positively correlated ($P < 0.05$), while CH with CA and UC; CA with LG, LP, and PA; TN with LG, LP, and UC; and PA with UC were negatively correlated ($P < 0.05$; Figure 2d). The PCA analysis and significant negative correlations indicated the DOM molecular trade-offs.[2] In this study, the sampling time was set 10−20 days after harvest to avoid external carbon input

https://doi.org/10.1021/acs.est.2c01137
Environ. Sci. Technol. 2022, 56, 11827−11834

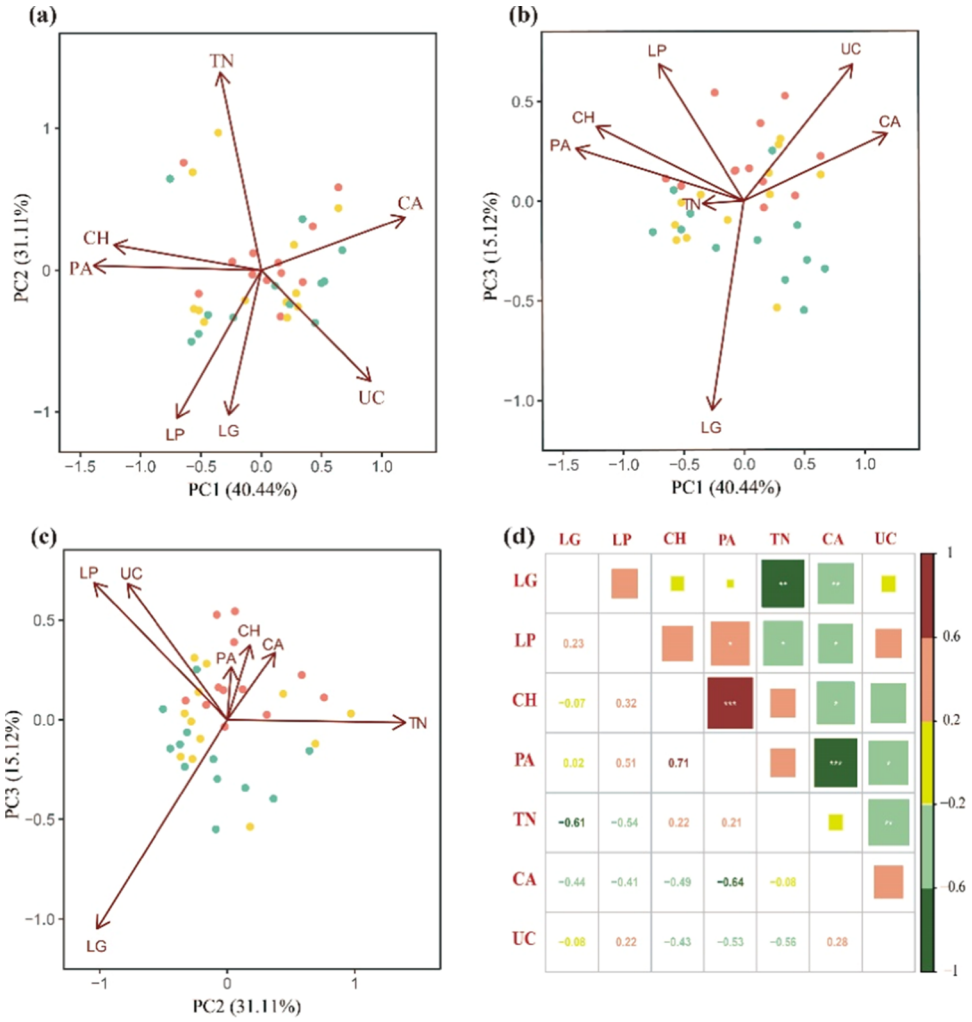

Figure 2. PCA and correlation heatmap of DOM compound groups. (a–c) PC1, PC2, and PC3 axes explained 40.44, 31.11, and 15.12% of the total variation in the correlation matrix of DOM molecule relative abundances, respectively. The dots represent the soil samples and colors refer to different fertilization practices (red – no fertilizers, yellow – mineral fertilizers, and green – mineral fertilizers plus organic amendments). (d) Correlation heatmap of the DOM molecule relative abundance within all samples. The symbols *, **, and **** indicate corrected at $P < 0.05$, $P < 0.01$, and $P < 0.001$, respectively; the correlation r values are also displayed; red color means positive correlation ($r > 0$), and green color means negative correlation ($r < 0$). A darker color indicates a higher r value.

from rice root or external disturbance caused by fertilizers. Thus, the molecular trade-offs in DOM at this stage reflected the variation results of different DOM molecules after long-term artificial cultivation in paddy ecosystems.

In a previous research study, Hall et al.[2] found three trade-off relationships (carbohydrate–char, carbohydrate–lipids, and lignin–protein) in soil organic matters based on ^{13}C NMR spectroscopy. In ^{13}C NMR, the compounds were identified by applying a molecular mixing model based on their carbon skeletons. In this study, the DOM molecules were identified by FT-ICR-MS and were grouped into different compounds based on their molecular formulas. Six types of compounds were identified in ^{13}C NMR and there were seven compound groups in FT-ICR-MS. Although some compound groups identified in ^{13}C NMR and FT-ICR-MS shared the same names (carbohydrate, lignin, lipid, and protein), the structural information they represented was not exactly the same. The trade-offs based on ^{13}C NMR essentially represented the increase or decrease of the content of different carbon components in SOC. Yet, trade-offs in FT-ICR-MS essentially represented the increase and decrease of molecular species in different DOM compound groups. Thus, the trade-offs found in this study are not the same as the results in ^{13}C NMR. Here, we found more trade-offs but they did not include the trade-offs of carbohydrate–lipids and lignin–protein in the ^{13}C NMR results. In ^{13}C NMR spectroscopy, char mainly represented the aromatic C and phenolic C.[29] Thus, char-like compounds in ^{13}C NMR were analogous to the aromatic-like (CA) compounds in FT-ICR-MS. Thus, the trade-off between CH and CA in this study is similar to the trade-off between carbohydrate and char in ^{13}C NMR results,[2] and they both indicated a quantitative exchange between liable and persistent compounds.

Potential Transforming Relationship of DOM Molecules. For all 7576 detected unique molecules, 65,998 trusted potential molecular transformations were found, and they could be grouped into transformations between any two compound groups (Figure 3 and Table S4). As there were seven compound groups, theoretically, 49 types of transformations between compound groups existed. In this study, 42 types of transformations were found, which included 7 intragroup transformations and 35 intergroup transformations

https://doi.org/10.1021/acs.est.2c01137
Environ. Sci. Technol. 2022, 56, 11827–11834

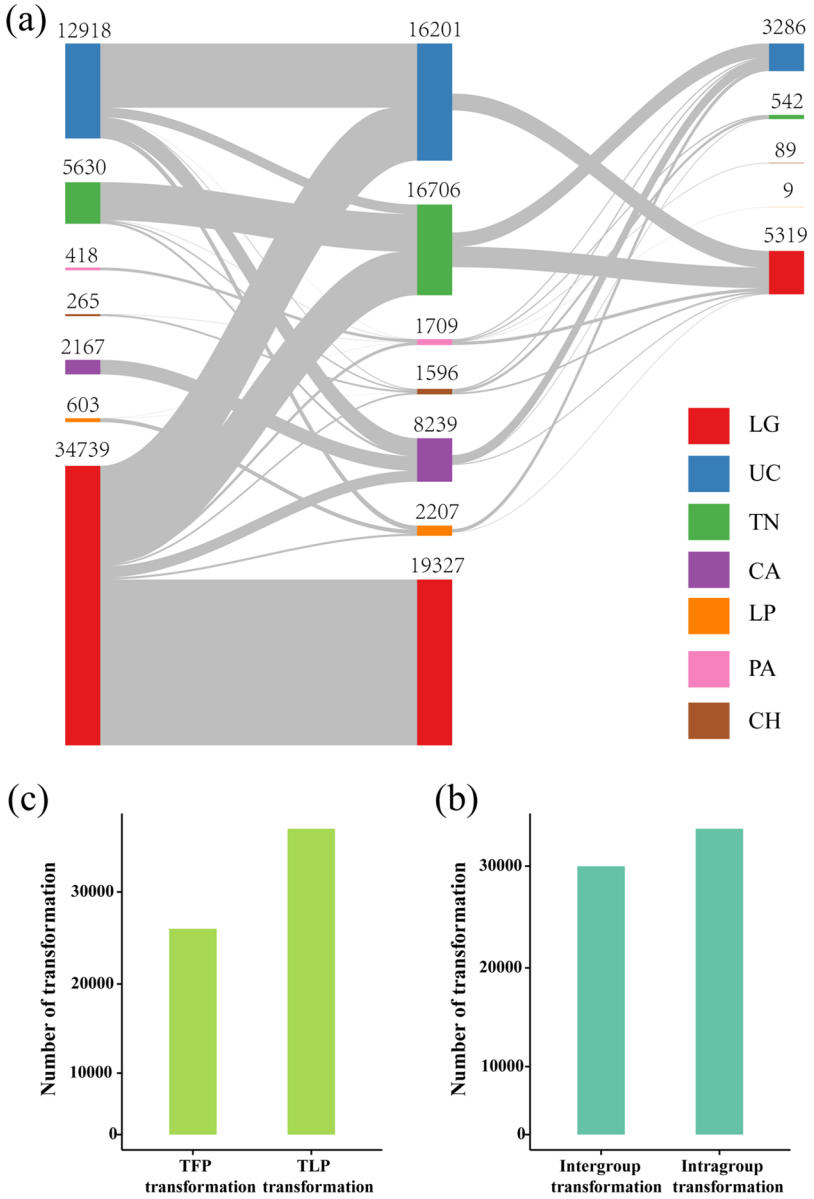

Figure 3. (a) Sankey diagram (with direction from left to right) showing the specific molecular transformations among the seven compound groups: different colors refer to different compound groups; the width of each flow is proportional to the number of a specific transformation and the height of each bar is proportional to the number of transformation in each group (the numbers are also shown). (b) The numbers of intergroup and intragroup transformations are shown. (c) The numbers of TFP and TLP transformations are shown. Intragroup transformation means the transformation occurring between the molecules in the same compound group, and intergroup transformation means the transformation occurring between different compound groups. TFP refers to thermodynamically favorable transformations and TLP refers to thermodynamically limited transformations.

(Table S4). Among all transformations, the TLP was more than the TFP transformation (Figure 3b), which indicated that more potential transformations required external forces or energy. In the long-term process of DOM formation and transformation, many forces, such as soil microbes, participated and finally led to the current existence state of the DOM molecules. Considering all transformations, intragroup transformation was more than intergroup transformation (Figure 3c). This indicated that the molecules within a compound group were more likely to undergo transformation than molecules between different compound groups. For a specific molecule, its transformation is more likely to be a loss of small fragments (intragroup) than a change in the molecular skeleton (intergroup).

For TFP, TLP, and all transformations, the more molecules there were in a compound group, the more molecular transformations the compound group was involved (Pearson's positive correlation with $P < 0.001$, Figure S1). Among all the different types of transformations, LG to LG accounted for the largest proportion, and the transformations of the top five all belonged to the transformations among LG, UC, and TN (Figure 3a and Table S4). A compound group showed different transform features in different potential transformations. For example, LG preferred to transform to other compound groups (out-transform) in TLP and all transformations, while LG was more likely to be transformed from other compound groups in TFP transformation (Table S5). This means that LG tended to spontaneously increase in TFP

https://doi.org/10.1021/acs.est.2c01137
Environ. Sci. Technol. 2022, 56, 11827−11834

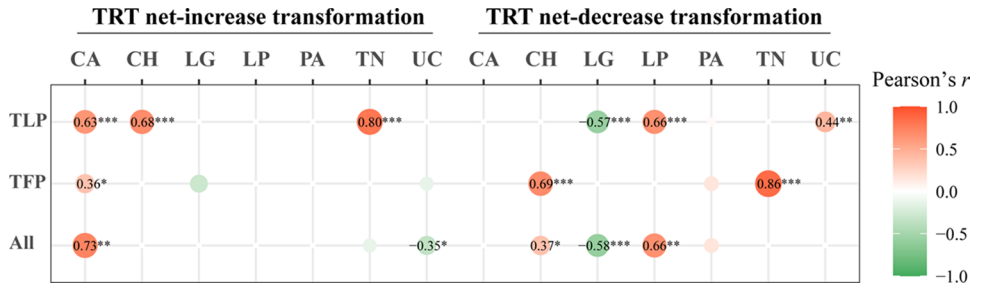

Figure 4. Relationship between the content of a compound group and its trade-off-related net transformation (net increase or net decrease) in all samples using linear mixed models. The circle presents Pearson's correlation and the *r* values are displayed if $P < 0.05$. The symbols *, **, and **** indicate corrected at $P < 0.05$, $P < 0.01$, and $P < 0.001$, respectively. The color indicates the direction of the relationship (red is positive and green is negative), and a darker color indicates a higher correlation coefficient. TRT, trade-off-related transformations; TFP, thermodynamically favorable transformations; TLP, thermodynamically favorable transformations; and All means all transformations including TFP and TLP.

transformation; however, LG is more likely to decrease when considering extra energies or forces (TLP and all transformations). Different compound groups also show different transformation features. CA and UC were always likely to be transformed from other compound groups in all three transformation processes (all, TFP, and TLP). CH, LP, and PA were likely to increase in TFP transformation and decrease in TLP transformation. In contrast, TN was likely to decrease in TFP transformation and increase in TLP transformation. Generally, the number and characteristics of molecules dictated the transform features of a compound group and these transform features also reflected the chemical activity of this compound group.

Molecular Trade-Offs in DOM Dictated by Potential Transformation of Molecules. The trade-offs between compounds reflect the variation of their relative contents, which is essentially the opposite trend of their relative contents. Transformation refers to the disappearance or appearance of a molecule based on biochemical reactions. The contents and trade-off relationships of the compound groups in DOM are the results of molecular transformations, exchanges with other soil organic matter (SOM) pools, and deriving from plant littler and dead microbial cells. Once the compounds go into the DOM pool, they experience molecular evolution. During molecular evolution, some DOM molecules constantly disappear (biochemistry transformation or adsorption to undissolved components) and others are created (biochemistry transformation or releasing from other pools), that is, molecular transformations always exist, which is similar to the continuum model for SOM.[30] Thus, the reasons for a trade-off relationship may be: (1) the two compounds have direct transformation; (2) they have transformation relationships with other compounds in the DOM pool; and (3) they are affected by external factors (including exchanges with other pools) and produced the opposite trend. For example, it was found that physico-chemical protection mechanisms could explain the increased relative abundance of carbohydrate, and when physico-chemical protection was lacking, char-like compounds (CA in this study) increased.[2] It meant that physico-chemical protection imposed opposite effects on the contents of CH and CA, and trade-offs between them were probably just the representations of their content variations. Our result also confirmed that no direct transformations existed between CH and CA; thus, transformation with other compounds or the physico-chemical protection may contribute to the trade-off between CH and CA.

For the seven compound groups, nine trade-off relationships were found: CA−CH, CA−LG, CA−LP, CA−PA, CH−UC, LG−TN, LP−TN, PA−UC, and TN−UC. By calculating all transformations related to a specific compound group, we could evaluate whether the molecule number in this group will be potentially increased or decreased through molecular transformations. In the TLP transformation process, CA, TN, and UC tended to experience net-increase transformation (in-transform > out-transform), while CH, LG, LP, and PA tended to experience net-decrease transformation (in-transform < out-transform) (Table S5). The two groups (net-increase compounds and net-decrease compounds) naturally showed trade-off relationships in the view of biochemical transformations. Thus, the above nine trade-offs except TN−UC could all be explained by the molecular transformations in the TLP process. In the TFP transformation process, TN tended to experience net-decrease transformation and other compounds did the opposite (Table S5). Thus, the molecular transformations could explain only three trade-offs (TN−LG, TN−LP, and TN−UC) in the TFP process, while in the all-transformation process, CA, LP, and UC tended to experience net-increase transformation and LG, PA, and TN did the opposite (Table S5). Thus, the molecular transformations could also explain five trade-offs (CA−LG, CA−PA, LP−TN, PA−UC, and TN−UC) in the all-transformation process. Briefly, all the nine trade-offs could be explained by molecular transformations, and the TLP transformation showed the best interpretation. A new viewpoint emphasized the simultaneous changes in energy and molecules, and energy demand was the main force of microorganisms to utilize plant litter to form SOMs.[31] Our result also demonstrated that the molecular transformations involving external energies or forces played a critical role in the DOM molecule formation and their trade-off relationships. Of course, it is worth noting that although TFP transformation can be spontaneous, it does not mean that there is no external involvement such as soil microbiome. Similarly, besides external energies and biotic factors, the catalytic reactions or physico-chemical protection may also facilitate the molecular transformations in the TLP process. Anyway, in the view of thermodynamics, TLP certainly needs more external energies or forces than the TFP process.

It has been shown that the trade-offs could be explained by molecular transformations; however, whether direct reciprocal biochemistry transformation between two compounds could explain their trade-off relationship needs further discussion. For the above nine trade-off relationships, CA−CH, CA−LP, and CA−PA could not be detected in the potential molecular

https://doi.org/10.1021/acs.est.2c01137
Environ. Sci. Technol. 2022, 56, 11827−11834

transformations, indicating that these three relationships did not have basis of a biochemistry reaction. This meant that CA could not directly transform to or be transformed from CH, LP, or PA. Thus, the trade-offs CA−CH, CA−LP, and CA−PA could be explained by their transformation relationships with other compounds rather than their direct transformations. The other six trade-offs CA−LG, CH−UC, LG−TN, LP−TN, PA−UC, and TN−UC all had biochemical bases (11 transformations highlighted in Table S4). These trade-off-related transformations (TRTs) directly correspond to the trade-offs of the compound contents. For a specific compound group, its TRT could be further classified as net-increase transformation (in-transform > out-transform) or net-decrease transformation. To test whether the TRT relationships could explain the content variations of a specific compound group, Pearson's correlation analysis was conducted (Figure 4). If the content of a compound group was significantly positively correlated with its net-increase TRT, logically, this TRT could explain the content variation of the compound group (more net increase to this compound led to its content increase). Similarly, if a compound content was significantly negatively correlated with its net-decrease TRT, logically, this TRT could also explain the content variation of the compound group (more net decrease to this compound led to its content decrease). However, if a compound content was negatively correlated with its net-increase TRT, this TRT and the content variation could not be explained by each other. If a compound content was significantly positively correlated with its net-decrease TRT, logically, the content of the compound group could explain its TRT variation (more content of a compound group indicated more potential out-transform for it).

In the TLP transformation, the contents of CA, CH, and TN were positively correlated ($P < 0.05$) with their net-increase TRT, and LG was negatively correlated ($P < 0.05$) with its net-decrease TRT (Figure 4). Thus, the TRT in TLP transformation could explain the content variations of CA, CH, TN, and LG, while the TRT could only explain the content variation of CA in the TFP transformation. In all-transformation, only the TRT of CA and LG could explain their content variations, and the contents of CH and LP could explain their corresponding net-decrease TRT transformations. The results indicated that the content variations of CA, CH, TN, and LG could be explained by their respective trade-off-related direct transformations under the control of external energies or forces.

Overall, this study revealed the molecular trade-offs of soil DOM at a regional scale. The potential molecular transformations of different compound groups were also evaluated using an optimized identification method. This study was the first to explain the trade-offs of DOM molecules using potential molecular transformations. Among all the seven compound groups in DOM, nine trade-offs were found and they could all be explained by direct or indirect molecular transformations. Six of the nine trade-offs had biochemical bases and these trade-off-related direct transformations could explain the content variations of CA, CH, TN, and LG. This indicated that molecular trade-offs in DOM had molecular transformation bases, and we can use molecular transformations to understand the content variations of different compound groups. It is worth noting that only the thermodynamically limited molecular transformations could well explain the molecular trade-offs and content variations. The results indicated that external energies played a critical role in forming the molecular trade-offs, and it also inspired us that using external forces impacts the DOM molecular transformation and organic carbon cycles in paddy fields.

■ ASSOCIATED CONTENT

Supporting Information

The Supporting Information is available free of charge at https://pubs.acs.org/doi/10.1021/acs.est.2c01137.

Transformation database (XLSX)

Basic information of long-term experimental stations; chemical properties of sampled soils; percentage of the compound number in each biomolecular compound group in different samples; every type of molecular transformation between different compound groups and their corresponding transformation numbers; the number of different types of transformations related to each compound group; linear regression between the molecule number and the number of molecular transformation (PDF)

■ AUTHOR INFORMATION

Corresponding Author

Zhongpei Li − *State Key Laboratory of Soil and Sustainable Agriculture, Institute of Soil Science, Chinese Academy of Sciences, Nanjing 210008, P. R. China*; Email: zhpli@issas.ac.cn

Authors

Meng Wu − *State Key Laboratory of Soil and Sustainable Agriculture, Institute of Soil Science, Chinese Academy of Sciences, Nanjing 210008, P. R. China*; orcid.org/0000-0003-2388-9546

Pengfa Li − *College of Life Sciences, Nanjing Agricultural University, Nanjing 210095, P. R. China*

Guilong Li − *State Key Laboratory of Soil and Sustainable Agriculture, Institute of Soil Science, Chinese Academy of Sciences, Nanjing 210008, P. R. China*

Kai Liu − *State Key Laboratory of Soil and Sustainable Agriculture, Institute of Soil Science, Chinese Academy of Sciences, Nanjing 210008, P. R. China*

Guozhen Gao − *State Key Laboratory of Soil and Sustainable Agriculture, Institute of Soil Science, Chinese Academy of Sciences, Nanjing 210008, P. R. China*

Shiyu Ma − *College of Life Sciences, Henan Agricultural University, Zhengzhou 450046, P. R. China*

Cunpu Qiu − *Zhenjiang College, Zhenjiang 212028, P. R. China*

Complete contact information is available at: https://pubs.acs.org/10.1021/acs.est.2c01137

Notes

The authors declare no competing financial interest.

■ ACKNOWLEDGMENTS

This work was supported by the National Key R&D Program of China (Project number: 2021YFD1500300), the National Natural Science Foundation of China (Project number: 42077021), and the Natural Science Foundation of Jiangsu Province (Project number: BK20221005).

REFERENCES

(1) Lal, R. Soil carbon sequestration impacts on global climate change and food security. *Science* **2004**, *304*, 1623−1627.
(2) Hall, S. J.; Ye, C. L.; Weintraub, S. R.; Hockaday, W. C. Molecular trade-offs in soil organic carbon composition at continental scale. *Nat. Geosci.* **2020**, *13*, 687−692.
(3) Khan, S.; Chao, C.; Waqas, M.; Arp, H. P.; Zhu, Y. G. Sewage sludge biochar influence upon rice (Oryza sativa L) yield, metal bioaccumulation and greenhouse gas emissions from acidic paddy soil. *Environ. Sci. Technol.* **2013**, *47*, 8624−8632.
(4) Zhang, S.; Chen, Z.; Wen, Q.; Ma, J.; He, Z. Assessment of maturity during co-composting of penicillin mycelial dreg via fluorescence excitation-emission matrix spectra: characteristics of chemical and fluorescent parameters of water-extractable organic matter. *Chemosphere* **2016**, *155*, 358−366.
(5) He, X. S.; Xi, B. D.; Cui, D. Y.; Liu, Y.; Tan, W. B.; Pan, H. W.; Li, D. Influence of chemical and structural evolution of dissolved organic matter on electron transfer capacity during composting. *J. Hazard. Mater.* **2014**, *268*, 256−263.
(6) McAdams, B. C.; Aiken, G. R.; McKnight, D. M.; Arnold, W. A.; Chin, Y. P. High pressure size exclusion chromatography (HPSEC) determination of dissolved organic matter molecular weight revisited: accounting for changes in stationary phases, analytical standards, and isolation methods. *Environ. Sci. Technol.* **2018**, *52*, 722−730.
(7) Nebbioso, A.; Piccolo, A. Molecular characterization of dissolved organic matter (DOM): a critical review. *Anal. Bioanal. Chem.* **2013**, *405*, 109−124.
(8) Chen, Q.; Chen, F.; Gonsior, M.; Li, Y. Y.; Wang, Y.; He, C.; Cai, R. H.; Xu, J. X.; Wang, Y. M.; Xu, D. P.; Sun, J.; Zhang, T.; Shi, Q.; Jiao, N. Z.; Zheng, Q. Correspondence between DOM molecules and microbial community in a subtropical coastal estuary on a spatiotemporal scale. *Environ. Int.* **2021**, *154*, No. 106558.
(9) Maqbool, T.; Sun, M. M.; Chen, L.; Zhang, Z. H. Exploring the fate of dissolved organic matter at the molecular level in the reactive electrochemical ceramic membrane system using fluorescence spectroscopy and FT-ICR MS. *Water Res.* **2022**, *210*, No. 117979.
(10) Li, Y. G.; He, C.; Li, Z.; Zhang, Y. X.; Wu, B. C.; Shi, Q. Molecular transformation of dissolved organic matter in refinery wastewater. *Water Sci. Technol.* **2020**, *82*, 107−119.
(11) Liu, X. M.; Hou, Y.; Yu, Z.; Wang, Y. Q.; Zhou, S. G.; Jiang, B.; Liao, Y. H. Comparison of molecular transformation of dissolved organic matter in vermicomposting and thermophilic composting by ESI-FT-ICR-MS. *Environ. Sci. Pollut. Res.* **2020**, *27*, 43480−43492.
(12) Wang, H.; Lu, L.; Chen, H.; McKenna, A. M.; Lu, J.; Jin, S.; Zuo, Y.; Rosario-Ortiz, F. L.; Ren, Z. J. Molecular transformation of crude oil contaminated soil after bioelectrochemical degradation revealed by FT-ICR Mass Spectrometry. *Environ. Sci. Technol.* **2020**, *54*, 2500−2509.
(13) Chen, H.; Hou, A. X.; Corilo, Y. E.; Lin, Q. X.; Lu, J.; Mendelssohn, I. A.; Zhang, R.; Rodgers, R. P.; McKenna, A. M. 4 Years after the Deepwater Horizon Spill: Molecular Transformation of Macondo Well Oil in Louisiana Salt Marsh Sediments Revealed by FT-ICR Mass Spectrometry. *Environ. Sci. Technol.* **2016**, *50*, 9061−9069.
(14) Chu, Q. N.; Xue, L. H.; Wang, B. Y.; Li, D. T.; He, H. Y.; Feng, Y. F.; Han, L. F.; Yang, L. Z.; Xing, B. S. Insights into the molecular transformation in the dissolved organic compounds of agro-waste-hydrochars by microbial-aging using electrospray ionization Fourier transform ion cyclotron resonance mass spectrometry. *Bioresour. Technol.* **2021**, *320*, No. 124411.
(15) Zhang, B. L.; Wang, X. N.; Fang, Z. Y.; Wang, S.; Shan, C.; Wei, S.; Pan, B. C. Unravelling molecular transformation of dissolved effluent organic matter in UV/H2O2, UV/persulfate, and UV/chlorine processes based on FT-ICR-MS analysis. *Water Res.* **2021**, *199*, No. 117158.
(16) Graham, E. B.; Goldman, A. E.; Crump, A. R.; Goldman, A. E.; Bramer, L. M.; Arntzen, E.; Romero, E.; Resch, C. T.; Kennedy, D. W.; Stegen, J. C. Carbon inputs from riparian vegetation limit oxidation of physically bound organic carbon via biochemical and thermodynamic processes. *J. Geophys. Res.: Biogeosci.* **2017**, *122*, 3188−3205.
(17) Danczak, R. E.; Chu, R. K.; Fansler, S. J.; Goldman, A. E.; Graham, E. B.; Tfaily, M. M.; Toyoda, J.; Stegen, J. C. Using metacommunity ecology to understand environmental metabolomes. *Nat. Commun.* **2020**, *11*, 6369.
(18) Kögel-Knabner, I.; Amelung, W.; Cao, Z. H.; Fiedler, S.; Frenzel, P.; Jahn, R.; Kalbitz, K.; Kölbl, A.; Schloter, M. Biogeochemistry of paddy soils. *Geoderma* **2010**, *157*, 1−14.
(19) Knox, S. H.; Matthes, J. H.; Sturtevant, C.; Oikawa, P. Y.; Verfaillie, J.; Baldocchi, D. Biophysical controls on interannual variability in ecosystem-scale CO_2 and CH_4 exchange in a California rice paddy. *J. Geophys. Res.: Biogeosci.* **2016**, *121*, 978−1001.
(20) Luo, Y.; Xiao, M. L.; Yuan, H. Z.; Liang, C.; Zhu, Z. K.; Xu, J. M.; Kuzyakov, Y.; Wu, J. S.; Ge, T. D.; Tang, C. X. Rice rhizodeposition promotes the build-up of organic carbon in soil via fungal necromas. *Soil Biol. Biochem.* **2021**, *160*, No. 108345.
(21) Wu, M.; Li, P. F.; Li, G. L.; Petropoulos, E.; Feng, Y. Z.; Li, Z. P. The chemodiversity of paddy soil dissolved organic matter is shaped and homogenized by bacterial communities that are orchestrated by geographic distance and fertilizations. *Soil Biol. Biochem.* **2021**, *161*, No. 108374.
(22) Koch, B. P.; Dittmar, T. From mass to structure: an aromaticity index for high-resolution mass data of natural organic matter. *Rapid Commun. Mass Spectrom.* **2006**, *20*, 926−932.
(23) LaRowe, D. E.; Van Cappellen, P. Degradation of natural organic matter: a thermodynamic analysis. *Geochim. Cosmochim. Acta* **2011**, *75*, 2030−2042.
(24) Stegen, J. C.; Johnson, T.; Fredrickson, J. K.; Wilkins, M. J.; Konopka, A. E.; Nelson, W. C.; Arntzen, E. V.; Chrisler, W. B.; Chu, R. K.; Fansler, S. J.; Graham, E. B.; Kennedy, D. W.; Resch, C. T.; Tfaily, M.; Zachara, J. Influences of organic carbon speciation on hyporheic corridor biogeochemistry and microbial ecology. *Nat. Commun.* **2018**, *9*, 585.
(25) Boye, K.; Noël, V.; Tfaily, M M.; Bone, S. E.; Williams, K. H.; Bargar, J. R.; Fendorf, S. Thermodynamically controlled preservation of organic carbon in floodplains. *Nat. Geosci.* **2017**, *10*, 415−419.
(26) Zhang, J. C.; McKenna, A. M.; Zhu, M. Q. Macromolecular characterization of compound selectivity for oxidation and oxidative alterations of dissolved organic matter by manganese oxide. *Environ. Sci. Technol.* **2021**, *55*, 7741−7751.
(27) Li, X. M.; Sun, G. X.; Chen, S. C.; Fang, Z.; Yuan, H. Y.; Shi, Q.; Zhu, Y. G. Molecular chemodiversity of dissolved organic matter in paddy soils. *Environ. Sci. Technol.* **2018**, *52*, 963−971.
(28) Breitling, R.; Ritchie, S.; Goodenowe, D.; Stewart, M. L.; Barrett, M. P. Ab initio prediction of metabolic networks using Fourier transform mass spectrometry data. *Metabolomics* **2006**, *2*, 155−164.
(29) Baldock, J. A.; Masiello, C. A.; Gélinas, Y.; Hedges, J. I. Cycling and composition of organic matter in terrestrial and marine ecosystems. *Mar. Chem.* **2004**, *92*, 39−64.
(30) Lehmann, J.; Kleber, M. The contentious nature of soil organic matter. *Nature* **2015**, *528*, 60−68.
(31) Gunina, A.; Kuzyakov, Y. From energy to (soil organic) matter. *Glob. Change Biol.* **2022**, *28*, 2169−2182.

https://doi.org/10.1021/acs.est.2c01137
Environ. Sci. Technol. 2022, 56, 11827−11834